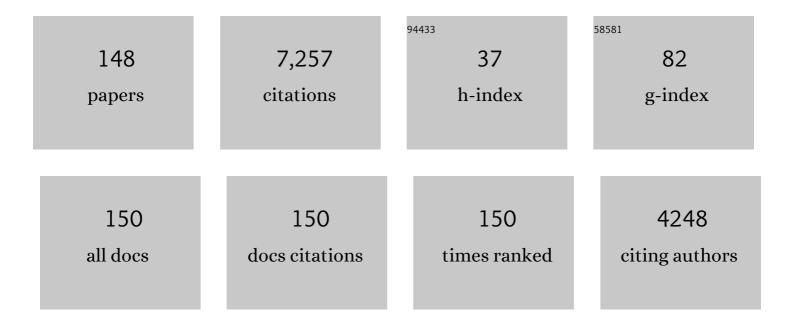
List of Publications by Year in descending order

Source: https://exaly.com/author-pdf/1099034/publications.pdf Version: 2024-02-01



REN COV

#	Article	IF	CITATIONS
1	High resolution 3D ultrasonic breast imaging by time-domain full waveform inversion. Inverse Problems, 2022, 38, 025008.	2.0	14
2	The IPASC data format: A consensus data format for photoacoustic imaging. Photoacoustics, 2022, 26, 100339.	7.8	6
3	High resolution 3D photoacoustic scanner for clinical vascular imaging: application to the assessment of inflammatory arthritis. , 2022, , .		1
4	Experimental evaluation of a 3-D fully convolutional network for learning blood oxygenation saturation using photoacoustic imaging. , 2022, , .		0
5	Broadband All-Optical Plane-Wave Ultrasound Imaging System Based on a Fabry–Perot Scanner. IEEE Transactions on Ultrasonics, Ferroelectrics, and Frequency Control, 2021, 68, 1007-1016.	3.0	13
6	Photoacoustic Reconstruction Using Sparsity in Curvelet Frame: Image Versus Data Domain. IEEE Transactions on Computational Imaging, 2021, 7, 879-893.	4.4	3
7	Modelling laser ultrasound waveforms: The effect of varying pulse duration and material properties. Journal of the Acoustical Society of America, 2021, 149, 2040-2054.	1.1	5
8	A Helmholtz equation solver using unsupervised learning: Application to transcranial ultrasound. Journal of Computational Physics, 2021, 441, 110430.	3.8	11
9	Ray-based inversion accounting for scattering for biomedical ultrasound tomography. Inverse Problems, 2021, 37, 115003.	2.0	9
10	Pyroelectric ultrasound sensor model: directional response. Measurement Science and Technology, 2021, 32, 035106.	2.6	2
11	Measurement of the ultrasound attenuation and dispersion in 3D-printed photopolymer materials from 1 to 3.5 MHz. Journal of the Acoustical Society of America, 2021, 150, 2798-2805.	1.1	15
12	Pseudospectral Time-Domain (PSTD) Methods for the Wave Equation: Realizing Boundary Conditions with Discrete Sine and Cosine Transforms. Journal of Theoretical and Computational Acoustics, 2021, 29, .	1.1	1
13	Transducer Module Development for an Open-Source Ultrasound Tomography System. , 2021, , .		3
14	The Effect of Curing Temperature and Time on the Acoustic and Optical Properties of PVCP. IEEE Transactions on Ultrasonics, Ferroelectrics, and Frequency Control, 2020, 67, 505-512.	3.0	7
15	100ÂMHz bandwidth planar laser-generated ultrasound source for hydrophone calibration. Ultrasonics, 2020, 108, 106218.	3.9	14
16	IPASC: a Community-Driven Consensus-Based Initiative Towards Standardisation in Photoacoustic Imaging. , 2020, , .		1
17	Nonlinear ultrasound simulation in an axisymmetric coordinate system using a <i>k</i> -space pseudospectral method. Journal of the Acoustical Society of America, 2020, 148, 2288-2300.	1.1	18
18	Stackable acoustic holograms. Applied Physics Letters, 2020, 116, .	3.3	21

#	Article	IF	CITATIONS
19	ElasticMatrix: A MATLAB toolbox for anisotropic elastic wave propagation in layered media. SoftwareX, 2020, 11, 100397.	2.6	11
20	Deep learning in photoacoustic tomography: current approaches and future directions. Journal of Biomedical Optics, 2020, 25, .	2.6	80
21	Toward accurate quantitative photoacoustic imaging: learning vascular blood oxygen saturation in three dimensions. Journal of Biomedical Optics, 2020, 25, .	2.6	41
22	Refraction-corrected ray-based inversion for three-dimensional ultrasound tomography of the breast. Inverse Problems, 2020, 36, 125010.	2.0	13
23	Test materials for characterising heating from HIFU devices using photoacoustic thermometry. , 2020, , .		1
24	Representing arbitrary acoustic source and sensor distributions in Fourier collocation methods. Journal of the Acoustical Society of America, 2019, 146, 278-288.	1.1	34
25	Analysis of the Directivity of Glass-Etalon Fabry–Pérot Ultrasound Sensors. IEEE Transactions on Ultrasonics, Ferroelectrics, and Frequency Control, 2019, 66, 1504-1513.	3.0	6
26	A pseudospectral method for solution of the radiative transport equation. Journal of Computational Physics, 2019, 384, 376-382.	3.8	10
27	The Influence of Strain-Optic Coefficients on the Transduction Mechanism of Planar Glass Etalon Fabry-Pérot Ultrasound Sensors. , 2019, , .		Ο
28	Measurement of the temperature-dependent speed of sound and change in Grüneisen parameter of tissue-mimicking materials. , 2019, , .		1
29	Reverberant cavity photoacoustic imaging. Optica, 2019, 6, 821.	9.3	12
30	Rapid calculation of acoustic fields from arbitrary continuous-wave sources. Journal of the Acoustical Society of America, 2018, 143, 529-537.	1.1	28
31	Model-Based Learning for Accelerated, Limited-View 3-D Photoacoustic Tomography. IEEE Transactions on Medical Imaging, 2018, 37, 1382-1393.	8.9	212
32	Effect of Backing on Carbon-Polymer Nanocomposite Sources for Laser Generation of Broadband Ultrasound Pulses. , 2018, , .		1
33	Accurate Time-Varying Sources in K-Space Pseudospectral Time Domain Acoustic Simulations. , 2018, , .		2
34	Enhancing Compressed Sensing 4D Photoacoustic Tomography by Simultaneous Motion Estimation. SIAM Journal on Imaging Sciences, 2018, 11, 2224-2253.	2.2	25
35	Equivalent-Source Acoustic Holography for Projecting Measured Ultrasound Fields Through Complex Media. IEEE Transactions on Ultrasonics, Ferroelectrics, and Frequency Control, 2018, 65, 1857-1864.	3.0	10
36	Three dimensional photoacoustic tomography in Bayesian framework. Journal of the Acoustical Society of America, 2018, 144, 2061-2071.	1.1	16

#	Article	IF	CITATIONS
37	Bandwidth-based mesh adaptation in multiple dimensions. Journal of Computational Physics, 2018, 371, 651-662.	3.8	1
38	Laser generated ultrasound sources using carbon-polymer nanocomposites for high frequency metrology. Journal of the Acoustical Society of America, 2018, 144, 584-597.	1.1	11
39	Approximate k-Space Models and Deep Learning for Fast Photoacoustic Reconstruction. Lecture Notes in Computer Science, 2018, , 103-111.	1.3	12
40	Nonstandard Fourier Pseudospectral Time Domain (PSTD) Schemes for Partial Differential Equations. Communications in Computational Physics, 2018, 24, .	1.7	8
41	Utilising the radiative transfer equation in quantitative photoacoustic tomography. , 2017, , .		2
42	Three-dimensional photoacoustic imaging and inversion for accurate quantification of chromophore distributions. , 2017, , .		5
43	Time domain reconstruction of sound speed and attenuation in ultrasound computed tomography using full wave inversion. Journal of the Acoustical Society of America, 2017, 141, 1595-1604.	1.1	78
44	Generating arbitrary ultrasound fields with tailored optoacoustic surface profiles. Applied Physics Letters, 2017, 110, .	3.3	40
45	Sensitivity of simulated transcranial ultrasound fields to acoustic medium property maps. Physics in Medicine and Biology, 2017, 62, 2559-2580.	3.0	69
46	Sub-sampled Fabry-Perot photoacoustic scanner for fast 3D imaging. Proceedings of SPIE, 2017, , .	0.8	8
47	Photoacoustic imaging with a multi-view Fabry-PÃ ${ m O}$ rot scanner. , 2017, , .		1
48	Accurate simulation of transcranial ultrasound propagation for ultrasonic neuromodulation and stimulation. Journal of the Acoustical Society of America, 2017, 141, 1726-1738.	1.1	103
49	Acoustic Wave Field Reconstruction From Compressed Measurements With Application in Photoacoustic Tomography. IEEE Transactions on Computational Imaging, 2017, 3, 710-721.	4.4	22
50	Mesh Density Functions Based on Local Bandwidth Applied to Moving Mesh Methods. Communications in Computational Physics, 2017, 22, 1286-1308.	1.7	5
51	Design of multi-frequency acoustic kinoforms. Applied Physics Letters, 2017, 111, .	3.3	37
52	Investigating the effect of thickness and frequency spacing on multi-frequency acoustic kinoforms. , 2017, , .		1
53	Staircase-free acoustic sources for grid-based models of wave propagation. , 2017, , .		0
54	Statistical independence in nonlinear model-based inversion for quantitative photoacoustic tomography. Biomedical Optics Express, 2017, 8, 5297.	2.9	2

#	Article	IF	CITATIONS
55	Laser generated ultrasound sources using polymer nanocomposites for high frequency metrology. , 2017, , .		0
56	Notice of Removal: Design of multi-frequency acoustic kinoforms. , 2017, , .		1
57	Laser generated ultrasound sources using polymer nanocomposites for high frequency metrology. , 2017, , .		Ο
58	Staircase-free acoustic sources for grid-based models of wave propagation. , 2017, , .		1
59	Exploiting statistical independence for quantitative photoacoustic tomography. , 2017, , .		1
60	Modeling Photoacoustic Propagation in Tissue Using k-Space Techniques. , 2017, , 25-34.		5
61	Estimation and uncertainty quantification of optical properties directly from the photoacoustic time series. , 2017, , .		Ο
62	Photoacoustic imaging using an 8-beam Fabry-Perot scanner. Proceedings of SPIE, 2016, , .	0.8	21
63	Characterisation of a phantom for multiwavelength quantitative photoacoustic imaging. Physics in Medicine and Biology, 2016, 61, 4950-4973.	3.0	39
64	Direct Estimation of Optical Parameters From Photoacoustic Time Series in Quantitative Photoacoustic Tomography. IEEE Transactions on Medical Imaging, 2016, 35, 2497-2508.	8.9	35
65	Independent component analysis for unmixing multi-wavelength photoacoustic images. , 2016, , .		2
66	Quantitative photoacoustic tomography using forward and adjoint Monte Carlo models of radiance. Journal of Biomedical Optics, 2016, 21, 126004.	2.6	36
67	Control of broadband optically generated ultrasound pulses using binary amplitude holograms. Journal of the Acoustical Society of America, 2016, 139, 1637-1647.	1.1	19
68	Accelerated high-resolution photoacoustic tomography via compressed sensing. Physics in Medicine and Biology, 2016, 61, 8908-8940.	3.0	112
69	Photoacoustic tomography using orthogonal Fabry–Pérot sensors. Journal of Biomedical Optics, 2016, 22, 041009.	2.6	24
70	Advanced photoacoustic image reconstruction using the k-Wave toolbox. Proceedings of SPIE, 2016, , .	0.8	10
71	Full-wave attenuation reconstruction in the time domain for ultrasound computed tomography. , 2016, , .		4
72	Image reconstruction with noise and error modelling in quantitative photoacoustic tomography. , 2016, , .		1

#	Article	IF	CITATIONS
73	Orthogonal Fabry-PÃ $\ensuremath{\mathbb{O}}$ rot sensors for photoacoustic tomography. , 2016, , .		2
74	PO-0937: Sound speed reconstruction in full wave ultrasound computer tomography for breast cancer detection. Radiotherapy and Oncology, 2016, 119, S454-S455.	0.6	0
75	Single pulse illumination of multi-layer photoacoustic holograms for patterned ultrasound field generation. , 2016, , .		2
76	On the adjoint operator in photoacoustic tomography. Inverse Problems, 2016, 32, 115012.	2.0	79
77	Bayesian parameter estimation in spectral quantitative photoacoustic tomography. , 2016, , .		1
78	Multispectral reconstruction methods for quantitative photoacoustic tomography. , 2016, , .		2
79	Sensitivity of quantitative photoacoustic tomography inversion schemes to experimental uncertainty. Proceedings of SPIE, 2016, , .	0.8	0
80	Single-pixel optical camera for video rate ultrasonic imaging. Optica, 2016, 3, 26.	9.3	66
81	A monitor function for spectral moving mesh methods applied to nonlinear acoustics. AIP Conference Proceedings, 2015, , .	0.4	0
82	Forward and adjoint radiance Monte Carlo models for quantitative photoacoustic imaging. , 2015, , .		1
83	Reconstruction-classification method for quantitative photoacoustic tomography. Journal of Biomedical Optics, 2015, 20, 126004.	2.6	11
84	Orthogonal Fabry-Pérot sensor array system for minimal-artifact photoacoustic tomography. , 2015, , .		4
85	Deep in vivo photoacoustic imaging of mammalian tissues using a tyrosinase-based genetic reporter. Nature Photonics, 2015, 9, 239-246.	31.4	362
86	Characterisation of a PVCP-based tissue-mimicking phantom for quantitative photoacoustic imaging. Proceedings of SPIE, 2015, , .	0.8	9
87	Quantitative photoacoustic tomography using illuminations from a single direction. Journal of Biomedical Optics, 2015, 20, 036015.	2.6	21
88	Effect of wavelength selection on the accuracy of blood oxygen saturation estimates obtained from photoacoustic images. , 2015, , .		8
89	A real-time ultrasonic field mapping system using a Fabry Pérot single pixel camera for 3D photoacoustic imaging. Proceedings of SPIE, 2015, , .	0.8	4
90	Super-resolution ultrasound. Nature, 2015, 527, 451-452.	27.8	36

#	Article	IF	CITATIONS
91	Characterisation of a PVCP based tissue-mimicking phantom for Quantitative Photoacoustic Imaging. , 2015, , .		5
92	The use of acoustic reflectors to enlarge the effective area of planar sensor arrays. , 2014, , .		1
93	Accuracy of approximate inversion schemes in quantitative photoacoustic imaging. , 2014, , .		4
94	Patterned interrogation scheme for compressed sensing photoacoustic imaging using a Fabry Perot planar sensor. Proceedings of SPIE, 2014, , .	0.8	2
95	Control of optically generated ultrasound fields using binary amplitude holograms. , 2014, , .		7
96	Modeling power law absorption and dispersion in viscoelastic solids using a split-field and the fractional Laplacian. Journal of the Acoustical Society of America, 2014, 136, 1499-1510.	1.1	46
97	Modelling elastic wave propagation using the k-Wave MATLAB Toolbox. , 2014, , .		55
98	Quantifying numerical errors in the simulation of transcranial ultrasound using pseudospectral methods. , 2014, , .		6
99	Photoacoustic imaging using acoustic reflectors to enhance planar arrays. Journal of Biomedical Optics, 2014, 19, 126012.	2.6	25
100	A Bayesian approach to spectral quantitative photoacoustic tomography. Inverse Problems, 2014, 30, 065012.	2.0	45
101	Photoacoustic tomography in a reflecting cavity. Proceedings of SPIE, 2013, , .	0.8	1
102	A gradient-based method for quantitative photoacoustic tomography using the radiative transfer equation. Inverse Problems, 2013, 29, 075006.	2.0	108
103	Bayesian Image Reconstruction in Quantitative Photoacoustic Tomography. IEEE Transactions on Medical Imaging, 2013, 32, 2287-2298.	8.9	48
104	3D quantitative photoacoustic tomography using the $\hat{\rm l}$ -Eddington approximation. Proceedings of SPIE, 2013, , .	0.8	5
105	Photoacoustic tomography in a rectangular reflecting cavity. Inverse Problems, 2013, 29, 125010.	2.0	19
106	A computationally efficient elastic wave model for media with power-law absorption. , 2013, , .		4
107	Image reconstruction in quantitative photoacoustic tomography using the radiative transfer equation and the diffusion approximation. , 2013, , .		0
108	A first-order <i>k</i> -space model for elastic wave propagation in heterogeneous media. Journal of the Acoustical Society of America, 2012, 132, 1271-1283.	1.1	59

#	Article	IF	CITATIONS
109	In vivo photoacoustic imaging of mouse embryos. Journal of Biomedical Optics, 2012, 17, 061220.	2.6	71
110	Quantitative spectroscopic photoacoustic imaging: a review. Journal of Biomedical Optics, 2012, 17, 061202.	2.6	550
111	In vivo preclinical photoacoustic imaging of tumor vasculature development and therapy. Journal of Biomedical Optics, 2012, 17, 1.	2.6	260
112	Plane wave ultrasound imaging with a broadband photoacoustic source. , 2012, , .		3
113	Reconstructing absorption and scattering distributions in quantitative photoacoustic tomography. Inverse Problems, 2012, 28, 084009.	2.0	74
114	Quantitative thermoacoustic image reconstruction of conductivity profiles. Proceedings of SPIE, 2012, , .	0.8	3
115	Modeling nonlinear ultrasound propagation in heterogeneous media with power law absorption using a <i>k</i> -space pseudospectral method. Journal of the Acoustical Society of America, 2012, 131, 4324-4336.	1.1	372
116	Effects of Saliva on Starch-thickened Drinks with Acidic and Neutral pH. Dysphagia, 2012, 27, 427-435.	1.8	37
117	In vivo preclinical photoacoustic imaging using all-optical detection and time-reversal image reconstruction. , 2012, , .		0
118	Estimating optical absorption, scattering, and Grueneisen distributions with multiple-illumination photoacoustic tomography. Applied Optics, 2011, 50, 3145.	2.1	70
119	Multimodal photoacoustic and optical coherence tomography scanner using an all optical detection scheme for 3D morphological skin imaging. Biomedical Optics Express, 2011, 2, 2202.	2.9	166
120	A <i>k</i> -space Green's function solution for acoustic initial value problems in homogeneous media with power law absorption. Journal of the Acoustical Society of America, 2011, 129, 3652-3660.	1.1	28
121	Multiple-illumination photoacoustic tomography: reconstructing absorption, scattering, and GrÃ1/4 eneisen coefficient distributions. , 2011, , .		0
122	In vivo longitudinal photoacoustic imaging of subcutaneous tumours in mice. Proceedings of SPIE, 2011, , .	0.8	5
123	Measurement of the Ultrasound Attenuation and Dispersion inÂWhole Human Blood and its Components From 0–70 MHz. Ultrasound in Medicine and Biology, 2011, 37, 289-300.	1.5	67
124	Acoustic attenuation compensation in photoacoustic tomography: application to high-resolution 3D imaging of vascular networks in mice. Proceedings of SPIE, 2011, , .	0.8	8
125	Time Domain Simulation of Harmonic Ultrasound Images and Beam Patterns in 3D Using the k-space Pseudospectral Method. Lecture Notes in Computer Science, 2011, 14, 363-370.	1.3	15
126	Photoacoustic tomography in absorbing acoustic media using time reversal. Inverse Problems, 2010, 26, 115003.	2.0	248

#	Article	IF	CITATIONS
127	Artifact Trapping During Time Reversal Photoacoustic Imaging for Acoustically Heterogeneous Media. IEEE Transactions on Medical Imaging, 2010, 29, 387-396.	8.9	74
128	Effect of sensor directionality on photoacoustic imaging: a study using the k-wave toolbox. Proceedings of SPIE, 2010, , .	0.8	8
129	Modeling power law absorption and dispersion for acoustic propagation using the fractional Laplacian. Journal of the Acoustical Society of America, 2010, 127, 2741-2748.	1.1	237
130	k-Wave: MATLAB toolbox for the simulation and reconstruction of photoacoustic wave fields. Journal of Biomedical Optics, 2010, 15, 021314.	2.6	1,501
131	Quantitative determination of chromophore concentrations from 2D photoacoustic images using a nonlinear model-based inversion scheme. Applied Optics, 2010, 49, 1219.	2.1	101
132	Quantitative Photoacoustic Image Reconstruction using Fluence Dependent Chromophores. Biomedical Optics Express, 2010, 1, 201.	2.9	25
133	Quantitative Photoacoustic Tomography with Fluence-Dependent Absorbers. , 2010, , .		1
134	The challenges for quantitative photoacoustic imaging. Proceedings of SPIE, 2009, , .	0.8	99
135	Estimating chromophore distributions from multiwavelength photoacoustic images. Journal of the Optical Society of America A: Optics and Image Science, and Vision, 2009, 26, 443.	1.5	150
136	Photoacoustic tomography with a single detector in a reverberant cavity. Journal of the Acoustical Society of America, 2009, 125, 1426-1436.	1.1	27
137	Modeling Photoacoustic Propagation in Tissue Using k-Space Techniques. Optical Science and Engineering, 2009, , 25-34.	0.1	4
138	Photoacoustic tomography using reverberant field data from a single detector. Proceedings of SPIE, 2008, , .	0.8	1
139	Simultaneous estimation of chromophore concentration and scattering distributions from multiwavelength photoacoustic images. Proceedings of SPIE, 2008, , .	0.8	4
140	Gradient-based quantitative photoacoustic image reconstruction for molecular imaging. , 2007, , .		20
141	k-space propagation models for acoustically heterogeneous media: Application to biomedical photoacoustics. Journal of the Acoustical Society of America, 2007, 121, 3453.	1.1	203
142	Photoacoustic tomography with a limited-aperture planar sensor and a reverberant cavity. Inverse Problems, 2007, 23, S95-S112.	2.0	89
143	Quantitative photoacoustic image reconstruction for molecular imaging. , 2006, , .		7
	Quantitative photoacoustic imaging: fitting a model of light transport to the initial pressure		

¹⁴⁴ Quantitative photoacoustic imaging: fitting a model of light transport to the initial pressur distribution., 2005,,.

#	Article	IF	CITATIONS
145	Generating photoacoustic signals using high-peak power pulsed laser diodes. , 2005, , .		33
146	Fast calculation of pulsed photoacoustic fields in fluids usingk-space methods. Journal of the Acoustical Society of America, 2005, 117, 3616-3627.	1.1	169
147	Fabry Perot polymer film fibre-optic hydrophones and arrays for ultrasound field characterisation. Journal of Physics: Conference Series, 2004, 1, 32-37.	0.4	20
148	The Rayleigh-like collapse of a conical bubble. Journal of the Acoustical Society of America, 2000, 107, 130-142.	1.1	40